JOURNAL OF MATERIALS SCIENCE **34** (1999) 5581–5588

Kinetics of formation of nanocrystalline phases by mechanochemical reaction between Ti and RuO_2

M. BLOUIN, D. GUAY*
INRS-Énergie et Matériaux, 1650 Blvd. Lionel-Boulet, C.P. 1020, Varennes, Québec, Canada J3X 1S2
E-mail: guay@inrs-ener.uquebec.ca

R. SCHULZ
Technologies Émergentes de production et de stockage, Institut de recherche d'Hydro-Québec, 1800 Blvd. Lionel-Boulet, C.P. 1000, Varennes, Québec, Canada J3X 1S1

The structural evolution of a mixture of Ti and RuO_2 mechanically alloyed over a period of 40 h was followed with respect to time by X-Ray diffraction. The structural parameters were extracted from the XRD traces by performing a Rietveld refinement analysis. The phase formation occurs in three distinct stages. In stage I (first 10 min of milling), RuO_2 and Ti reacts to form RuTi, Ru, and TiO, with some other oxide phases of titanium (Ti_2O_3, and TiO_2). In stage II (between 10 and 60 min), the reaction slows down and the titanium dioxides are being reduced. In stage III, decomposition of RuTi through reaction with Ti_2O_3 occurs, to yield to the formation of TiO and Ru. In stage I, the reaction rate is very high, for example, 34.7 wt % of RuTi is formed after only 10 min of milling. It is argued that such rapid reaction rate is due to the enthalpy of the redox reaction occurring between Ti and RuO_2 which raised the local temperature and thus favors the atomic interdiffusion. Finally, a series of experiments performed as a function of the milling intensity points to the existence of an energy threshold below which the combustion reaction between Ti and RuO_2 does not occur.

1. Introduction

The production of sodium chlorate is an energy consuming process. Typically, the overpotential of the electrolysis step is larger than 900 mV. This large overpotential exists in spite of several efforts to develop activated electrodes for both sides of the reaction.

Over the years, the anodic overpotential at the typical current density of 250 mA cm^{-2} or more has dropped from about 400 to 50 mV with the advent of the well-known Dimensionally Stable Anodes (DSA®) [1]. Therefore, the anodic overpotential accounts for about 5% of the total overpotential of the electrolysis step. On the cathodic side, where hydrogen evolution occurs, highly efficient and stable activated cathodes still need to be found. In the industry, steel cathodes are used, with an overpotential of more than 800 mV, and the situation is even worse in the case of Ti cathodes. Important energy savings and cost reduction could be gained by lowering the cathodic overpotential. For example, a reduction of 300 mV would result in a reduction of the total energy consumption by about 10%.

It was shown elsewhere that good electrocatalytic properties for hydrogen evolution in typical chlorate electrolysis conditions could be achieved by using a nanocrystalline alloy obtained by milling a powder mixture of Ti, Ru and Fe [2]. The X-ray analysis showed that a cubic structure (cP2-CsCl), corresponding to Ti_2RuFe, was formed after extensive milling [2].

However, during a prolonged operation of electrolysis, these electrodes suffer from decrepitation [3, 4, 5]. To overcome this problem, oxygen was added to the alloy. The mechanical stability was greatly improve [3, 4, 5] while no effect was observed on the activity of the material [6, 7]. For example, an alloy containing about 12 wt % of oxygen (Ti_2RuFeO_2) can withstand more than 150 h of electrolysis in typical electrolysis conditions without displaying a sign of degradation [3, 4, 5].

There are several ways of adding O to the nanocrystalline alloy. Pre-formed Ti_2RuFe can be exposed to an O_2 containing atmosphere during the milling process. As shown elsewhere [6], this leads to the decomposition of the simple cubic structure (Ti_2RuFe), with the formation of Ru, Fe and TiO. It is also possible to introduce O in the alloy by using an oxide in the initial powder mixture. However, in that case, the reaction

* Author to whom all correspondence should be addressed.

path and the composition of the final products depend on the nature of the oxide, as does the kinetics of the reaction [8].

In this paper, we focus our attention on an initial mixture of Ti and RuO_2 only. This binary system was chosen because the oxides of Ti and Ru have the largest difference in the free energies of formation among TiO_2, Fe_2O_3 and RuO_2. There has been some debate in the literature regarding the evaluation of the local temperature increase during the milling process and its importance in determining structural evolution. In particular, the effect of deformations and shear bands on local heating have been discussed [9, 10, 11]. Recently, the effect of the reaction enthalpy on the local temperature rise was also recognized [12]. When reduction of a metal oxide occurs during the milling, this effect can overwhelmed all the others. For example, the melting of Cu was evidenced during the milling of CuO and Al [12]. Therefore, we expect a large driving force for the oxido-reduction reaction to take place and a significant increase of the local temperature during the milling of Ti with RuO_2 because of the reaction enthalpy.

This paper study a mixture of Ti and RuO_2 at various stages of milling. The structural investigation was performed by X-Ray diffraction and Rietveld refinement analysis. The effect of the milling energy on the structural evolution was also analyzed. It will be shown that the milling process occurs in three distinct stages. In the first one, an increase of the local temperature as a result of the reaction enthalpy causes the rapid formation of the cubic (RuTi) structure, Ru and some oxide phases. In the second stage the reaction slows down considerably and some titanium oxide phases are being reduced. In the third stage, RuTi decomposes, homogenization takes place and the system evolves to a final state of TiO and Ru. It will also be shown that the proportion of each phase at the end of the process depends on the energy of milling.

2. Experimental

Pure Ti and RuO_2 powders (99.5% or higher) from Micron and Alfa-Aesar, respectively, were used as starting materials. In all cases, the powders were mixed in the initial proportion $2Ti + 1RuO_2$. The milling experiments were performed in a short (interior diameter: 381 mm, length: 476 mm) or a long (interior diameter: 381 mm, length: 486 mm) steel crucible, with two 11 mm diameter and one 14 mm diameter balls. The ball to powder weight ratio was kept constant at about 4.5/1. Both a Spex 8000 mixer/mill and a modified paint mixer allowing variation of the amplitude of the movement were used. In a first set of experiments, the effect of the milling time on the structure of the powder was assessed by using the Spex 8000 with the long crucible. Small amounts of powder were taken at selected milling times for analysis. In a second set of experiments, the powders were milled 40 h using various crucibles and milling equipment to vary the energy of the milling process. All manipulations were performed under a controlled Ar atmosphere in a glove box to prevent oxygen or nitrogen contamination.

X-ray diffraction (XRD) diagrams were taken on a Siemens D-500 or a Philips X'PERT diffractometer using the CuK_α radiation. The XRD traces were analyzed by the Rietveld method [13], using the GSAS software [14]. Scanning electron microscopy (SEM) and Energy Dispersive X-Ray (EDX) spectroscopy were obtained using a Hitachi S-570 Scanning Electron Microscope (15 kV) with a Noran detector.

3. Results

3.1. Effect of the milling time

The XRD patterns of a powder mixture ($2Ti + RuO_2$) are shown in Fig. 1 as a function of milling time. Quantitative information regarding (i) the weight fractions phases; (ii) the crystal sizes; and (iii) the lattice parameters were obtained from such XRD traces by performing Rietveld refinement analyses (see Table I). Up to nine phases were identified and the principal reflections of each phase are shown on Fig. 1. These phases are: Ti (hP2-Mg), RuO_2 (tP6-TiO_2), Ru (hP2-Mg), RuTi (cP2-CsCl), TiO (cF8-NaCl), Ti_2O_3 (hR10-Al_2O_3), TiO_2 in its rutile form (tP6-TiO_2), TiO_2 in its anatase form (tI12-TiO_2), and Fe (cI2-W) which comes from the wear of the crucible.

The variation of the weight fraction of the various phases is shown in Fig. 2 as a function of the milling time. For milling time exceeding 1500 min, the proportion of each phase in the powder remains unchanged. The characteristic features to be emphasized are:

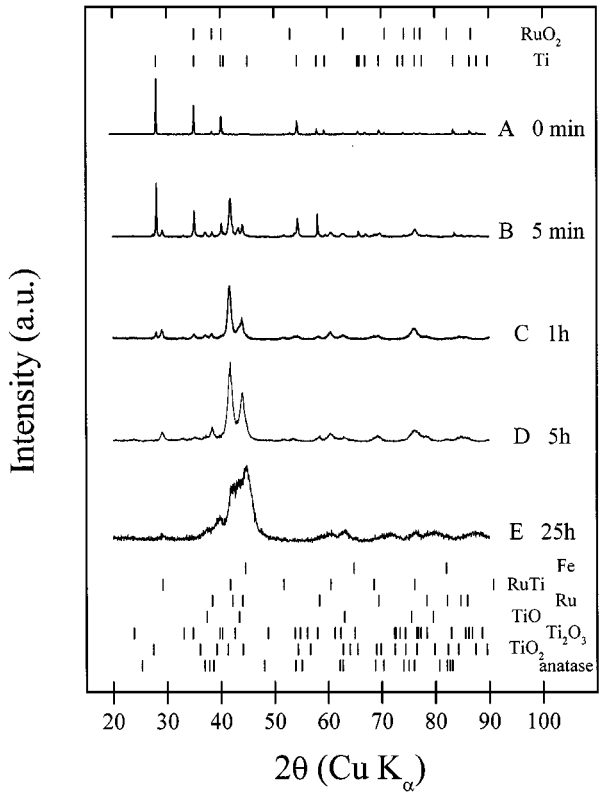

Figure 1 X-Ray diffraction patterns of a mixture of $2Ti + RuO_2$ as a function of milling time: (a) $t = 0$, (b) $t = 5$ min, (c) $t = 60$ min, (d) $t = 300$ min, and (e) $t = 1500$ min. The peak positions of the phases in the powder are also shown.

TABLE I Structural parameters of the ball-milled Ti-RuO_2 powder mixture

Milling time (min)	Phase	Lattice Parameters a (Å)	c (Å)	Crystallite size (nm)	Phase concentration (wt %)
5	RuTi	3.058		25	30.5
	RuO_2	4.491	3.106	>100	24.7
	Ru	2.704	4.286	31	8.7
	TiO	4.185		29	20.2
	Ti_2O_3	5.152	13.626	59	6.8
	TiO_2 (rutile)	4.597	2.992	8	9.1
10	RuTi	3.064		38	34.7
	RuO_2	4.485	3.101	>100	7.2
	Ru	2.707	4.275	40	8.9
	TiO	4.181		53	24.4
	Ti_2O_3	5.144	13.616	20	15.1
	TiO_2 (anatase)	3.808	9.505	34	1.7
	TiO_2 (rutile)	4.591	2.974	12	7.9
25	RuTi	3.067		33	37.2
	RuO_2	4.491	3.103	88	5.9
	Ru	2.711	4.278	39	12.2
	TiO	4.185		39	23.8
	Ti_2O_3	5.154	13.631	19	10.0
	TiO_2 (anatase)	3.895	8.447	39	0.7
	TiO_2 (rutile)	4.597	2.993	8	10.2
45	RuTi	3.066		15	38.2
	RuO_2	4.495	3.102	27	4.0
	Ru	2.708	4.304	17	14.0
	TiO	4.179		13	20.8
	Ti_2O_3	5.115	13.745	5	18.1
	TiO_2 (rutile)	4.633	2.865	8	4.9
60	RuTi	3.067		28	40.6
	RuO_2	4.507	3.108	24	5.6
	Ru	2.710	4.301	19	13.8
	TiO	4.185		17	21.9
	Ti_2O_3	5.100	13.835	6	18.0
900	RuTi	3.053		10	20.0
(15 h)	Ru	2.681	4.304	7	23.4
	TiO	4.195		4	31.0
	Fe	2.919		4	25.6
1500	RuTi	3.049		8	12.7
(25 h)	Ru	2.639	4.259	5	37.5
	TiO	4.182		7	26.6
	Fe	2.904		5	23.2

(i) The rapid drop of the weight fractions of RuO_2 and Ti at the beginning of the milling. Indeed, the weight fraction of Ti is already beyond the detection limit after 5 min of milling while that of RuO_2 has decreased from 58.1 to 24.7 wt % during this period of time;

(ii) The formation of several new phases. After 5 min of milling, significant proportion of RuTi, Ru and TiO are observed along with non-negligible amount of Ti_2O_3 and TiO_2;

(iii) The appearance of Fe after a long milling time, which arises as a result of the attrition of the steel balls and crucible.

In Fig. 2, we can distinguish four patterns in the variation of the weight fractions: (α) for Ti_2O_3, TiO_2 anatase and TiO_2 rutile, the weight fractions first increase, pass through a maximum then decrease to zero. In the case of Ti_2O_3, the weight fraction does not vanish before 300 min of milling; (β) for Ru and TiO, the weight fractions just kept increasing with milling time; (χ) for RuTi, the weight fraction first goes through a maximum and then decreases to reach a non-zero value after extensive milling; (δ) finally, in the case of RuO_2 and Ti, the weight fraction decreases from their initial values to zero rapidly in the first 10 min then more slowly afterward.

The reaction proceeds in three stages. Stage I occurs at the very beginning of the process and is characterized by a rapid change in weight fractions and the formation of RuTi and Ti oxide phases. Stage II occurs at milling times between 10 and 60 min, and is characterized by a much slower rate of variation of the weight fractions and the reduction of the highly oxidized Ti species. Finally in the third stage RuTi disappears and the system evolves slowly to a stable state composed of Ru and TiO. Obviously, the chemical and physical phenomenon governing these stages are different.

The total Ru, Ti and O contents, calculated from the values of the weight fraction of each phase deduced from the Rietveld refinement analysis are given in Table II. The expected value for the Ru, Ti and O contents, based on the nominal composition of the initial powder mixture, is 44.16, 41.86 and 13.98 wt %, respectively. The agreement between the calculated and the expected values is quite good. The error is the largest initially (5 and 10 min) because the main diffraction peaks of Ti, located at $2\Theta = 35.065^\circ$ (1 0 0), 38.404°

TABLE II Total atomic content as a function of milling time[a]

Milling time (min)	Total Ru content (wt %)	Total Ti content (wt %)	Total O content (wt %)
5	48.2	34.9	16.9
10	38.0	45.3	16.7
25	41.9	43.0	15.1
45	43.0	42.8	14.2
60	45.7	41.5	12.9
300	45.1	42.2	12.7
Mean	43.7	41.6	14.8

[a]These values were calculated from the phase composition of the powder obtained from the Rietveld refinement analysis. The expected values for the Ru, Ti and O contents, based on the nominal composition of the initial powder mixture, are 44.16, 41.86 and 13.98 wt %, respectively.

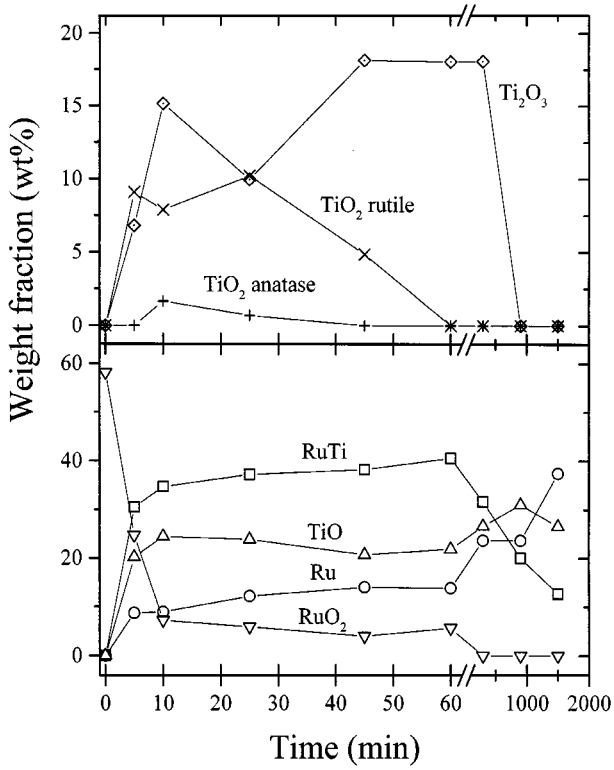

Figure 2 Evolution of the weight fractions of the various phases as a function of the milling time.

(0 0 2) and 40.151° (1 0 1), almost coincide with those of RuO_2 ((1 0 1) at 35.065° and (2 0 0) at 40.040°) and Ru ((1 0 0) at 38.387°). Nevertheless, the results indicate that the Rietveld refinement analysis is quite accurate.

The variation of the lattice parameters of Ru, TiO and RuTi is shown in Fig. 3 as a function of milling time. These phases were chosen because they are present throughout the whole milling process. The lattice parameter of RuTi evolves from 3.058 to about 3.065 Å as milling time goes from 5 to 60 min. These values are quite close to the expected value of 3.06 Å for that phase [15, 16]. In the Ti-Ru system, an intermetallic RuTi compound is formed over a very narrow range of composition near equiatomic concentration at equilibrium [15]. On the Ti-rich side of that narrow region, there is an immiscibility gap between β-Ti(Ru) and RuTi. However, as depicted elsewhere [2], the variation of the lattice parameter of β-Ti(Ru) with the Ru

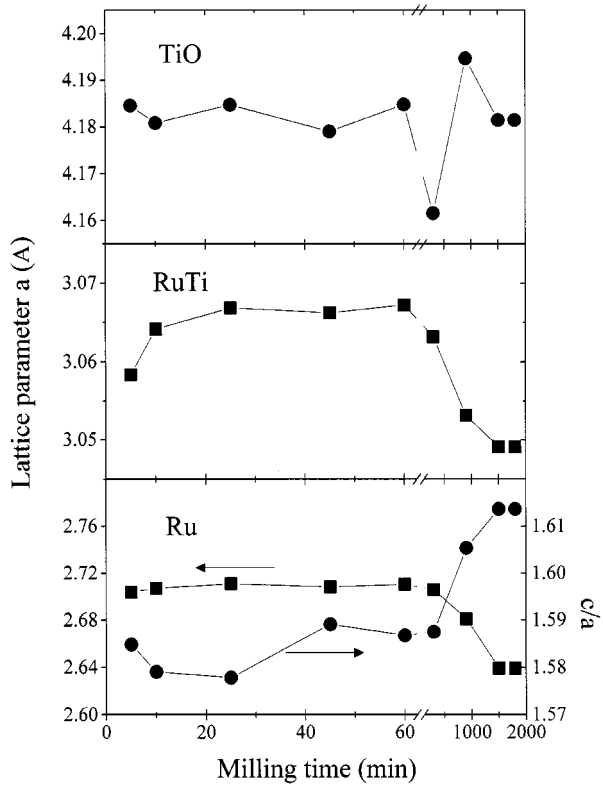

Figure 3 Evolution of the lattice parameters of RuTi, TiO and Ru as a function of the milling time.

content falls onto a straight line which reaches the lattice parameter of the equiatomic RuTi compound. So, assuming that milling allows the solubility range of Ru in β-Ti to be extended beyond its equilibrium value [17] so as to bridge the immiscibility gap between β-Ti(Ru) and TiRu, it would be possible to continuously vary the concentration of Ru solutes dissolved into β-Ti up to the equiatomic concentration. Such a phenomenon as already been observed in the case of other binary systems [18, 19]. In these conditions, values of lattice parameter larger than 3.06 Å indicate that the phase is enriched with Ti.

The RuTi cell volume starts to decrease after 60 min of milling. This is most probably related to the attrition of the balls and container and to the incorporation of Fe into the structure of RuTi. The covalent radius of Fe is smaller than Ru, so the lattice parameter shrinks [2]. Fe is isoelectronic with Ru, and the heat of mixing of Fe and Ru is lower (−7 kJ/mol [20]) than that of Fe and Ti (−25 kJ/mol [20]). So, replacement of Ru by Fe on the 1b site of the cubic structure is favored, as it was demonstrated elsewhere [2]. A similar effect as been observed in the case of RuAl ball-milled in steel crucible [21]. For milling times exceeding 1500 min, the value of the lattice parameter of RuTi(Fe) does not change anymore. The lattice parameters of FeTi is 2.976 Å, while that of RuTi is 3.06 Å. Assuming that Vegard's law holds true, the value of the lattice parameter of the cubic phase after extensive milling (3.049 Å) gives a final composition of $Ti_2Ru_{0.87}Fe_{0.13}$.

Likewise, the variation of the lattice parameter of Ru proceeds in two steps. For milling time less than 60 min, the Ru lattice parameter is almost constant. The "*a*" value lies between 2.70 and 2.71, while the

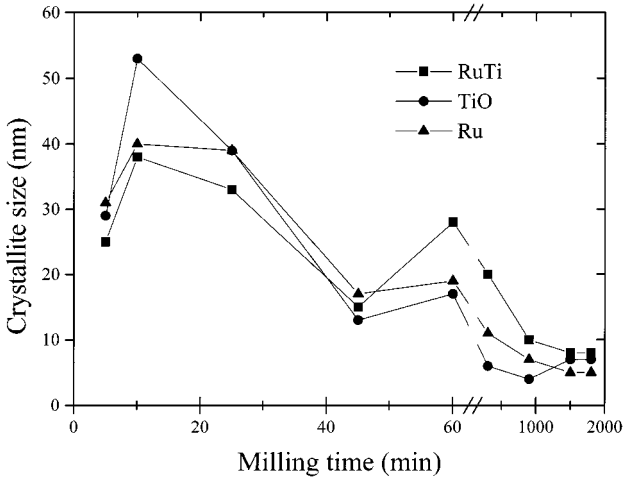

Figure 4 Evolution of the crystallite sizes of RuTi, Ru and TiO as a function of the milling time.

c/a ratio is between 1.58 and 1.59. The small discrepancy from the expected value is probably due to the presence of a small amount Ti dissolved in Ru. Indeed, the Ru-Ti phase diagram indicates that up to 10 at % of Ti can be introduced into the hexagonal structure of Ru, corresponding to a value of 2.71 and a "c/a" ratio of 1.59 [15]. For longer milling times, the lattice parameter of Ru decreases to reach a value of 2.64 Å after 1500 min of milling, while the c/a ratio increases to about 1.615 Å. As for RuTi, such a variation is probably related to the dissolution of Fe in hcp Ru.

Finally, the lattice parameter of TiO is almost constant at about 4.18 Å over the whole time domain. The lattice parameter of TiO_x is a function of the O content, varying from 4.20 to 4.17 as x in TiO_x varies from 0.7 to 1.3 [22]. So small fluctuations in the lattice parameter of TiO could be accounted for by small changes in stoichiometry. For example, variation of about 0.05 Å would be accounted for by a 5 at % variation of O in TiO (between $TiO_{0.9}$ and $TiO_{1.1}$).

The variation of the crystallite sizes of RuTi, Ru and TiO is shown in Fig. 4 as a function of the milling time. In general, the crystallite size decreases from about 40 to 5 nm except for two peaks located at the end of phase I and phase II. The phenomenon will be discuss later on.

3.2. Effect of the milling energy

In this series of experiments, milling was performed for a fixed period of time (40 h) while the energy imparted to the powder mixture was varied. This was done by changing the milling equipment (see the details in the experimental section). The XRD traces of the powders are shown in Fig. 5; traces A and B were obtained using the Spex 8000 mixer/mill with a long and short vial, respectively, while the small vial and the modified paint mixer were used for traces C (large motion amplitude) and D (small motion amplitude). Therefore curves A and C correspond to higher energy milling operation than curves B and D, respectively.

It can be seen from Fig. 5 that the proportion of each phase at the end of the milling process depends on the milling parameters. For instance, in curve A, the (1 1 0)

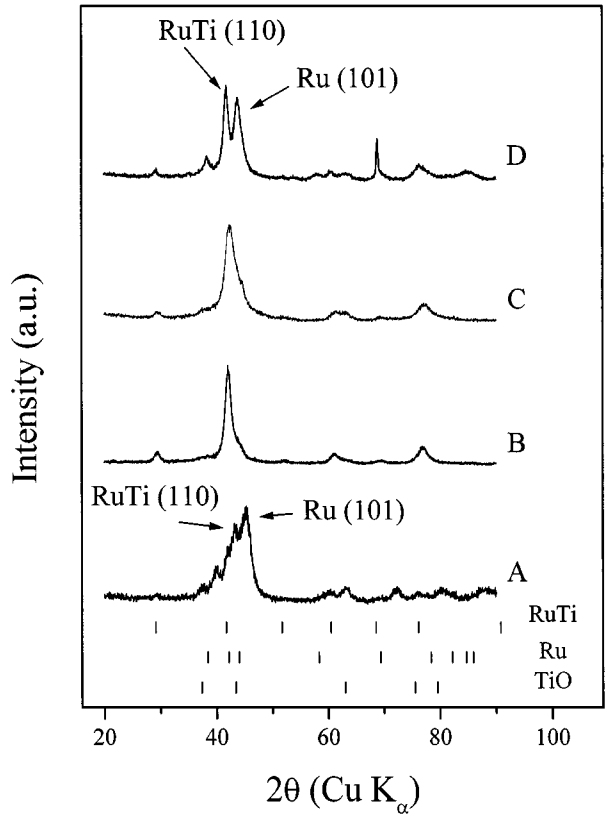

Figure 5 X-Ray diffraction patterns of a mixture of $2Ti + RuO_2$ milled 40 h. The milling energy was varied by using several combinations of milling equipment and crucibles.

peak of RuTi ($2\Theta = 41.71^\circ$) appears only as a faint shoulder in the three characteristic broad peaks of hcp Ru, while in curves B and C, the (1 1 0) reflections of cubic RuTi are dominant. In the case of curve D, the cubic and hcp phases have equivalent intensities.

Curve A of Fig. 5 is similar to curve E of Fig. 1. It was obtained after milling 40 h in the same conditions as in the first series of experiments. In these conditions, the structure of the phase mixture does not change much after 25 h of milling and is highly disordered. Decreasing the milling energy (curve B) has the effect of favoring the cubic structure (RuTi) over the hexagonal phase (Ru). Curves B and C are quite similar, which means that the milling intensity must be about the same. Decreasing the milling energy still further by reducing the motion amplitude of the crucible leads to a situation where the main diffraction peaks of RuTi and Ru have about the same intensity (curve D).

In curve A, the hcp Ru phase is dominant probably because the milling intensity is high enough to reach Phase III of the reaction within the 40 h time frame. In curves B and C, the milling energy is such that only Phase II of the reaction sequence has been reached in 40 h and therefore, the cubic RuTi prevails (see Fig. 2). In curve D, the milling intensity is probably so low that a self-sustaining combustion reaction never occurs.

4. Discussion

It has been shown previously that the milling of an elemental mixture of Ti + Ru + Fe leads to the formation

of Ti_2RuFe, which has a cubic structure (cP2, CsCl), with Ti atoms sitting preferentially on the 1a site and Ru or Fe atoms randomly distributed on the 1b site [2]. The cubic RuTi compound formed during the milling of Ti and RuO_2 is analogous to Ti_2RuFe, the only difference being the sharing of the 1b site by Ru and Fe atoms in the latter case. The formation of elemental Ru and various titanium oxide phases when oxygen is present was also expected from previous studies [6, 23].

What is interesting, however, in the first series of experiments is the rate at which RuTi is formed. This rate is strongly dependant on the nature and composition of the initial powder mixture. For example, in the case of the milling of an elemental mixture of 2Ti + Ru + Fe, the simple cubic phase (Ti_2RuFe) forms in about 3–6 h [2, 8]. This time period is of 5–10 h if a mixture of pre-milled TiO + Ti and Ru is used, and of 10–20 h in the case of a mixture of 2TiO + Ru [8]. For higher oxidation states of titanium (Ti_2O_3 or TiO_2) milled with Ru, the formation of the cubic structure is totally suppressed. In the present case (Ti + RuO_2), the weight fraction of RuTi is 30.5 wt % after 5 min of milling, which means more than an order of magnitude faster than in the previous cases. Therefore, the rate of formation of the cubic phase is slow when oxygen is provided by stable oxides (Ti) and fast when it is provided by less stable oxides (Ru).

In the case of a mixture of 2Ti + Ru + Fe, we observe in the early stage of the milling a structural transition from hcp-Ti to β-Ti (Ru, Fe) and then the cubic phase (Ti_2RuFe) is formed by solid state diffusion of Ru and Fe atoms in β-Ti. In the case of the mixture of Ti and

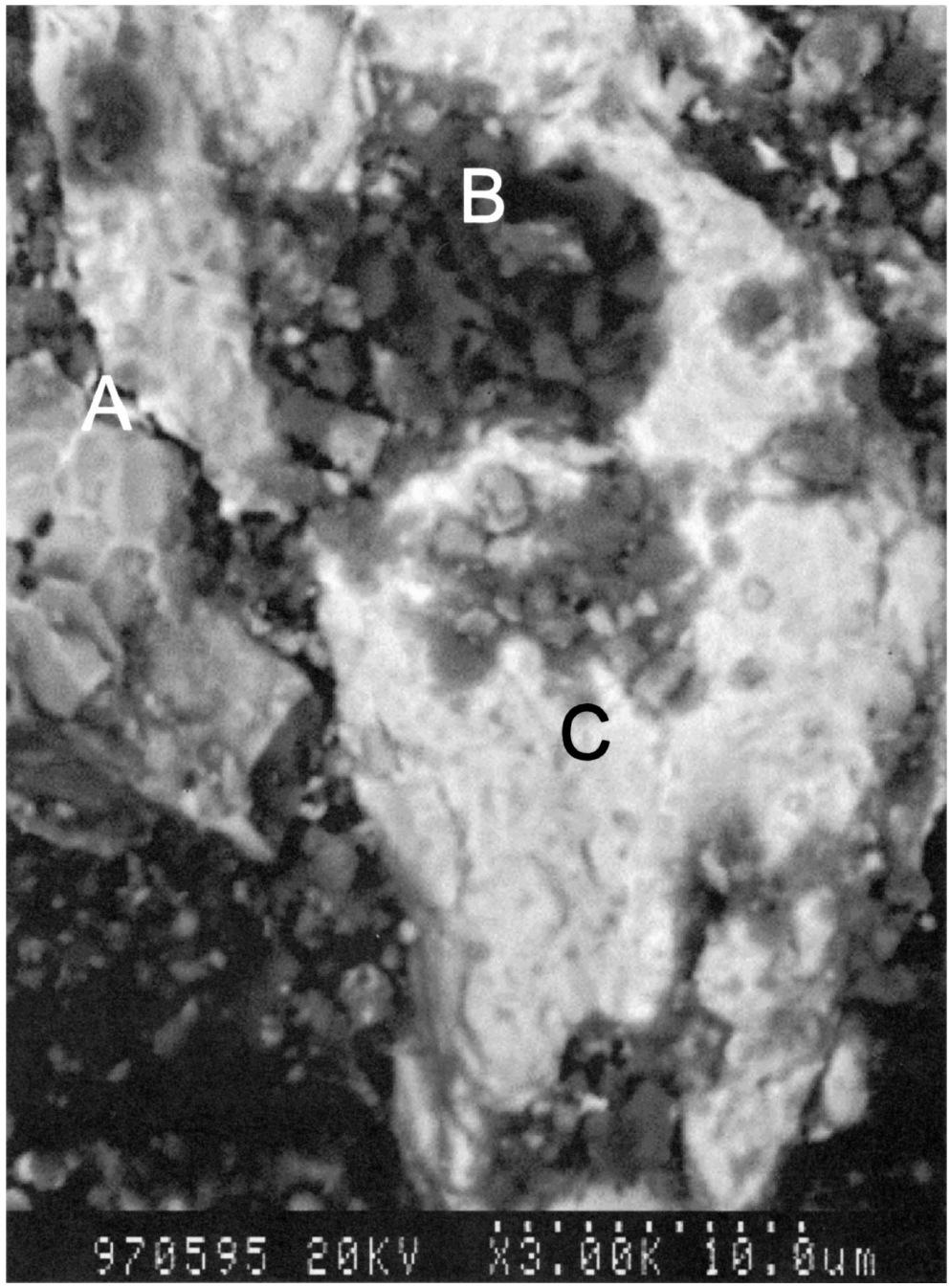

Figure 6 Scanning electron micrograph of a powder milled 10 min. The image was taken in backscattering electron mode. The magnification is 3000×.

RuO_2, the reaction rate is much faster and a different mechanism is at play, as evidenced by the reduction of RuO_2 and the oxidation of Ti. The enthalpy of the redox reaction which takes place between RuO_2 and Ti will cause an increase of the local temperature which favor atomic interdiffusion and even perhaps the melting of components if the enthalpy is high enough. To estimate the local temperature rise in the adiabatic approximation, we can use the following expression [12].

$$\Delta T_{\mathrm{ad}} = \left(\Delta H_{\mathrm{r}} - \sum \Delta H_{\mathrm{m}}\right) \Big/ \sum C_{\mathrm{p}}$$

where ΔH_{r} is the heat of the redox reaction, $\sum \Delta H_{\mathrm{m}}$ is the sum of heats of fusion of products which melt during the reaction and $\sum C_{\mathrm{p}}$ is the sum of heat capacities of the reaction products.

Assuming that the following reactions occurs in Phase I of the milling process,

$$\mathrm{Ti} + \mathrm{RuO_2} \rightarrow \mathrm{TiO_2} + \mathrm{Ru} \quad (1)$$

$$2\mathrm{Ti} + 3/2\ \mathrm{RuO_2} \rightarrow \mathrm{Ti_2O_3} + 3\mathrm{Ru} \quad (2)$$

$$2\mathrm{Ti} + \mathrm{RuO_2} \rightarrow 2\mathrm{TiO} + \mathrm{Ru} \quad (3)$$

$$2\mathrm{Ti} + \mathrm{RuO_2} \rightarrow \mathrm{TiO_2} + \mathrm{Ru}^* + \mathrm{Ti}^* \rightarrow \mathrm{TiO_2} + \mathrm{RuTi} \quad (4)$$

$$3\mathrm{Ti} + \mathrm{RuO_2} \rightarrow 2\mathrm{TiO} + \mathrm{Ru}^* + \mathrm{Ti}^* \rightarrow 2\mathrm{TiO} + \mathrm{RuTi} \quad (5)$$

We find $\Delta T_{\mathrm{ad}} = 8226$, 5586, 6687, 6110, and 5273 K, respectively. In each case, the adiabatic temperature rise is sufficiently high to melt the products, the melting points of Ru and RuTi being 2607 and 2403 K, respectively.

In these reaction models, the phases formed during a collision depend on the composition (Ti/RuO_2 ratio) of the powder mixture in the reaction volume. Obviously, this composition changes from one collision event (ball-powder-ball or ball-powder-container) to the other, which is why a variety of titanium oxide phases as well as both Ru and RuTi are formed.

A scanning electron micrograph of the powder obtained after 10 min of milling in shown in Fig. 6 (backscattering electron mode). The brighter regions are due to the heaviest elements (Ru), while the darker ones originate from the lighter elements (Ti). EDX analyses of region A reveal a mixed RuTi composition, indicating most probably the presence of RuTi. Regions B and C are Ti-and Ru-rich zones, respectively. There is no sign of melted regions in this micrograph however the temperature must have gone up substantially because the average crystal size of Ru, RuTi and TiO increases significantly in the first 10 min of milling. It has been shown that, self heating during the ball-milling of multicomponent systems that undergo a redox reaction may be such that the ignition temperature for self-sustain combustion reaction is reached [11, 24]. The time scale to reach the ignition temperature is of the order of 5–10 min in the case of the Zn-S system [25], and 2 h in the case of the Fe + CuO system [24]. For the $Ti + RuO_2$ system, the large enthalpy of the redox reaction favor a short incubation period comparable to the Zn-S case.

During the last stage of the milling process (stage III), one observes the disappearance of RuTi and TiO_2 and then Ti_2O_3. The most probable reaction is

$$\mathrm{RuTi} + \mathrm{Ti_2O_3} \rightarrow \mathrm{Ru} + 3\mathrm{TiO}$$

So, upon prolonged milling, the system tends towards a condition where all Ti atoms are in the +2 oxidation state. The situation is analogous to what has been found, when preformed Ti_2RuFe is milled in presence of O_2 [6]. In that case, decomposition of Ti_2RuFe occurred with the precipitation of Ru, Fe and TiO.

5. Conclusion

The structural evolution of a ball-milled mixture of 2Ti + RuO_2 was studied has a function of milling time. It was shown that the enthalpy of the redox reaction between Ti and RuO_2 rise the local temperature of the reaction volume substantially, thereby allowing fast interdiffusion and formation of the intermetallic compound RuTi and several Ti oxide phases. After only 10 min of milling, the weight fraction of RuTi reaches 35 wt %. In comparison, the closely related Ti_2RuFe phase is still undetected after 180 min of milling if a mixture of elemental (Ti, Ru and Fe) is used. In the second stage of the reaction, when there is basically no more reactants (Ti and RuO_2) left, TiO_2 is being reduced and the kinetics of the solid state reaction slows down. In the final stage of the reaction, decomposition of RuTi, formation of TiO and precipitation of Ru occur and the system evolves to a steady state.

Acknowledgement

This work was supported by the Natural Sciences and Engineering Research Council of Canada and Hydro-Québec. Marco Blouin also thanks FCAR-Québec for a student fellowship.

References

1. H. B. BEER, *J. Electrochem. Soc.* **127** (1980) 303C.
2. M. BLOUIN, D. GUAY, J. HUOT and R. SCHULZ, *J. Mater. Res.* **12** (1997) 1492.
3. D. GUAY, E. IRISSOU, L. ROUÉ, S.-H. YIP, M. BLOUIN, S. BOILY, J. HUOT and R. SCHULZ, Proc. 10th *International Forum on Electrolysis in the Chemical Industry:* Electrosynthesis CO, Lancaster, NY, 1996, p. 346.
4. L. ROUÉ, É. IRISSOU, A. BERCIER, S. BOUARICHA, M. BLOUIN, D. GUAY, S. BOILY, J. HUOT and R. SCHULZ, *J. Appl. Electrochem.* **29** (1999) 551.
5. S.-H. YIP, D. GUAY, S. JIN, E. GHALI, A. VAN NESTE and R. SCHULZ, *J. Mater. Res.* **13** (1998) 1171.
6. M. BLOUIN, D. GUAY and R. SCHULZ, *Nano. Mater.* **10** (1998) 523.
7. M. BLOUIN, D. GUAY, S. BOILY, A. VAN NESTE and R. SCHULZ, *Mater. Sci. Forum* **225-227** (1996) 801.
8. S.-H. YIP, D. GUAY, S. JIN, E. GHALI, A. VAN NESTE and R. SCHULZ, *J. Mater. Res.* **13** (1998) 1171.
9. A. YE. YERMAKOV, YE. YE. YURCHOKOV and V. A. BARINOV, *Phys. Met. Metall.* **52** (1981) 50.

10. R. B. SCHWARZ and C. C. KOCH, *Appl. Phys. Lett.* **49** (1986) 146.
11. R. M. DAVIS, B. MCDERMOTT and C. C. KOCH, *Met. Trans.* **19A** (1988) 2867.
12. G. B. SCHAFFER and P. G. MCCORMICK, *J. Mater. Sci. Let.* **9** (1990) 1014.
13. R. A. YOUNG, in "The Rietveld Method," edited by R. A. Young (Oxford University Press, Oxford, 1993) pp. 1–38.
14. A. C. LARSON and R. B. VON DREELE, "GSAS-general structure analysis system", Los Alamos National Laboratory Report No. LA-UR 86-748, 1986.
15. V. E. RAUB and E. RÖSCHEL, *Z. Metallkde* **54** (1963) 455.
16. C. B. JORDAN, *J. Metals* **7** (1955) 832.
17. R. RAY, B. C. GIESSEN and N. GRANT, *J. Metal. Trans.* **3** (1972) 627.
18. C. C. KOCH, *Ann. Rev, Mater. Sci.* **19** (1989) 121.
19. M. QI, M. ZHU and D. Z. YANG, *J. Mater. Sci. Lett.* **13** (1994) 966.
20. F. R. DE BOER, R. BOOM, W. C. M. MATTENS, A. R. MIEDEMA and A. K. NIESSEN, Cohesion in Metal (North-Holland Physics Publishing, New York, NY, 1989) p. 224.
21. H. J. FECHT, E. HELLSTERN, Z. FU and W.L. JOHNSON, Advances in Powder Metallurgy Vol. 2, (MPIF, Princeton, NJ, 1989) pp. 111–122.
22. M. D. BANUS, T. B. REED and J. STRAUSS, *Phys. Rev. B* **5** (1972) 2775.
23. M. BLOUIN, D. GUAY, J. HUOT, R. SCHULZ and I. P. SWAINSON, *J. Appl. Phys.* submitted.
24. T. D. SHEN, K. Y. WANG, J. T. WANG and M. X. QUAN, *Mater. Sci. Eng.* **A151** (1992) 189.
25. L. TAKACS and M. A. SUSOL, *Mater. Sci. Forum* **225-227** (1996) 559.

Received 19 February 1998
and accepted 8 February 1999